Geophysical Prospecting, 2001, **49**, 461–482

2D inversion of refraction traveltime curves using homogeneous functions

V.B. Piip*

Geological Department, Moscow State University, Vorobjevy Gory, 119899 Moscow, Russia

Received August 1997, revision accepted March 2001

ABSTRACT

A method using simple inversion of refraction traveltimes for the determination of 2D velocity and interface structure is presented. The method is applicable to data obtained from engineering seismics and from deep seismic investigations. The advantage of simple inversion, as opposed to ray-tracing methods, is that it enables direct calculation of a 2D velocity distribution, including information about interfaces, thus eliminating the calculation of seismic rays at every step of the iteration process. The inversion method is based on a local approximation of the real velocity cross-section by homogeneous functions of two coordinates. Homogeneous functions are very useful for the approximation of real geological media. Homogeneous velocity functions can include straight-line seismic boundaries. The contour lines of homogeneous functions are arbitrary curves that are similar to one another. The traveltime curves recorded at the surface of media with homogeneous velocity functions are also similar to one another. This is true for both refraction and reflection traveltime curves. For two reverse traveltime curves, non-linear transformations exist which continuously convert the direct traveltime curve to the reverse one and vice versa. This fact has enabled us to develop an automatic procedure for the identification of waves refracted at different seismic boundaries using reverse traveltime curves. Homogeneous functions of two coordinates can describe media where the velocity depends significantly on two coordinates. However, the rays and the traveltime fields corresponding to these velocity functions can be transformed to those for media where the velocity depends on one coordinate. The 2D inverse kinematic problem, i.e. the computation of an approximate homogeneous velocity function using the data from two reverse traveltime curves of the refracted first arrival, is thus resolved. Since the solution algorithm is stable, in the case of complex shooting geometry, the common-velocity cross-section can be constructed by applying a local approximation. This method enables the reconstruction of practically any arbitrary velocity function of two coordinates.

The computer program, known as GODOGRAF, which is based on this theory, is a universal program for the interpretation of any system of refraction traveltime curves for any refraction method for both shallow and deep seismic studies of crust and mantle.

Examples using synthetic data demonstrate the accuracy of the algorithm and its sensitivity to realistic noise levels. Inversions of the refraction traveltimes from the Salair ore deposit, the Moscow region and the Kamchatka volcano seismic profiles illustrate the methodology, practical considerations and capability of seismic imaging with the inversion method.

*E-mail: piipvalentina@hotmail.com

INTRODUCTION

Until 1960, the main methods used for investigating the crystalline basement and deep structures of the earth were those using refracted waves and at that time a huge amount of refraction data had been gathered from such seismic exploration. In particular, the territory of the former Soviet Union had been covered by a network of profiles of different characteristics. Refracted waves were used for investigating the oil basins in West Siberia, South Turkmenia, Bashkiria and other regions.

However, after 1960, the common-depth-point reflection method replaced refracted wave methods in seismic exploration and at the same time new interpretative methods based on a 2D model for refracted waves were investigated. Currently, the above methods – plus–minus and others – have been replaced by the following two methods: 2D modelling (ray tracing) and tomography using curved rays. At Moscow State University, a 2D method of inversion of refraction traveltime curves, i.e. the homogeneous function method, was proposed and was first used in the 1980s. The method is based on a local approximation of the real velocity distribution by homogeneous functions of two coordinates. Homogeneous functions are infinite-dimensional functions. In polar coordinates they are described by the product of two functions: a power function of any degree of the radius and an arbitrary function of the polar angle. Thus an infinite number of coefficients describe the homogeneous function in the case of a Taylor series. Ray-tracing methods are also based on local approximations of the real velocity distribution (Červený, Molotkov and Pšenčík 1977). For the local approximation, different functions can be used, e.g. a piecewise constant function (Ganzha 1982), a bilinear function (Boldyrev, Kaz and Ponomarev 1982) and quadratic fractional functions (Zelt and Smith 1992). For example, the dimension of velocity function used by Zelt and Smith (1992) is 7.

Ray-tracing and tomography methods as well as generalized linear inversion methods require an initial model and, in addition, the final velocity cross-section often depends on the initial model chosen. The construction of this initial model is time-consuming.

Inversion using homogeneous functions does not require an initial model and in addition the preliminary distinguishing and identification of waves on traveltime curves from different interfaces is unnecessary. It is performed automatically.

Tomography methods require a very detailed observation system, i.e. many shot and receiver locations, because the number of gridpoints where velocity values are calculated depends directly on the number of observations. In contrast to seismic experiments, which consist of numerous shots along a profile, it may be impossible through trial-and-error modelling to construct a model that fits the data within acceptable limits. The inversion method using the homogeneous function approximation is applicable to any set of traveltime curves, from the minimal case of two reverse traveltime curves to cases where the receivers and sources are equally spaced along the profile.

Homogeneous functions are not arbitrary functions of two coordinates. However, they are very suitable for the approximation of real geological media because they correspond to the properties of real seismic media. We know that the values of the horizontal components of real velocity gradients are much smaller than the values of the vertical component. The structure of homogeneous functions corresponds to this. Homogeneous functions in the radial direction change as a power function (i.e. a smooth function) but in the subvertical direction (depending on the polar angle) they can change arbitrarily and can have discontinuities (seismic boundaries).

The inversion method works well for the 2D case. For a homogeneous function of three coordinates, however, the solution of the inverse problem will require comprehensive analysis.

In its present form the inversion method does not include the use of full waveforms (i.e. traveltimes only), wide-angle reflection traveltimes and amplitudes of waves; however, these may be accommodated in the future.

Linear inversion and tomography methods using ray tracing are unstable and need a preliminary smoothing of boundaries. In contrast, the inversion algorithm using homogeneous functions is stable. This has been proved theoretically (Piip and Efimova 1987) and practically.

Special methods and tests to estimate the correlation of the level of detail or spatial resolution of a final cross-section to the geometry of given traveltime curves are used in ray-tracing and tomography methods. The spatial resolution of cross-sections calculated by the method using homogeneous functions corresponds to the data set in all cases. Using the inversion method with two reverse traveltime curves, we can obtain, in cross-section only, linear seismic boundaries and monotonic velocity functions in layers. The more detailed the data system, the more detailed the resulting cross-section can be.

Investigations show that the final velocity models obtained by the inversion method fit the observed times sufficiently well. The inversion process using the homogeneous function method requires less time and demands considerably less effort than other methods.

PROPERTIES OF HOMOGENEOUS FUNCTIONS

The inversion method is based on the local approximation of a real velocity cross-section by homogeneous functions of two coordinates (Piip 1978, 1982a,b, 1991). Homogeneous functions are a very wide class of infinite-dimensional functions, which are very useful for approximating real geological media. In polar coordinates, homogeneous functions are described by the product of two functions of a single coordinate – a power function of the radial coordinate and an arbitrary function of the polar angle:

$$v = r^m \psi(\varphi), \tag{1}$$

where m, the degree of the homogeneous function, is real. As $\psi(\varphi)$ is an arbitrary function, the seismic model described by the homogeneous function can include straight-line seismic boundaries (lines of discontinuity of function) and waveguides (layers) where velocity values decrease with depth. Contour lines of homogeneous functions are arbitrary but similar curves. This enables us to approximate layered geological media by homogeneous functions sufficiently well. We use the term 'similarity' in the following sense. Similar phenomena (physical fields, geometrical figures) are those for which a linear transformation of variables describing them produces coincident results.

This model was chosen because it affords the possibility of producing similar traveltime curves from sources situated at neighbouring points along a profile. For media that are homogeneous in the horizontal direction, the traveltime curves obtained from sources at different points on a profile are identical, but when widely different traveltime curves are obtained from neighbouring points on a profile, we must assume that there is a geological block boundary between these points. These are the two extreme cases. Usually the traveltime curves from neighbouring sources along a profile resemble one another, i.e. they have similar features, and the properties of the layered cross-sections in the horizontal direction change smoothly. Similarity may involve identity as a special case.

The ability of homogeneous velocity functions to give an approximate description of the character of geological media is illustrated below. The possible forms of the velocity fields described by a homogeneous function in two coordinates are shown in Fig. 1. The contours of the velocity fields of function (1) are as follows: $m = 0$ in the first column; $m > 0$ in the second column; $m < 0$ in the third column; the fourth column shows the corresponding graphs of the functions $\psi(\varphi)$. It can be seen that the main interpretative model, i.e. a two-layer model with constant velocities, is a special case of a homogeneous function class. A 1D inhomogeneous model can be obtained from (1) as a limiting case, as is shown below.

We define the domain of homogeneous functions by $0 < r < r_k$, $0 \leq \varphi < \pi/2$, because at the point $r = 0$, $\varphi = 0$, the velocity takes the non-physical value of zero. The problem of selecting the position of the origin is discussed below.

In order to illustrate the properties of the homogeneous functions and to show that a 1D inhomogeneous model is the limiting case of some homogeneous function, we consider the following. We compare the homogeneous function

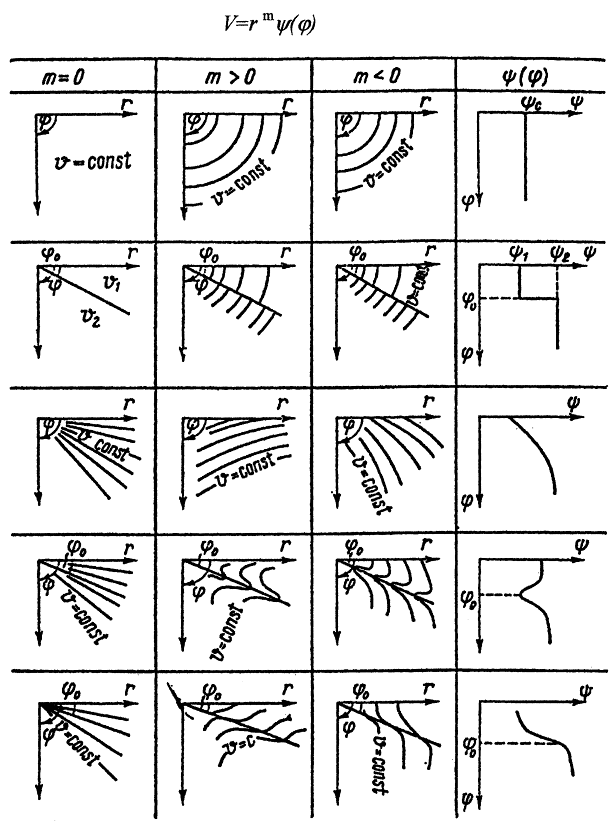

Figure 1 Possible forms of velocity fields and plots of $\psi(\phi)$ for homogeneous functions. The function $\psi(\phi)$ is an arbitrary function of the polar angle and may have discontinuities. Consequently velocity fields may contain linear seismic boundaries.

$v(r,\varphi)=r^m\psi(\varphi)$ and the function $v_1(x,z)=x^m f(z)$, where x and z are Cartesian coordinates and $f(z)$ is an arbitrary function of depth. We now use the Cartesian coordinates to represent the homogeneous function,

$$v(x,z) = (\sqrt{x^2 + z^2})^m(\arctan(z/x)).$$

We consider the homogeneous function in the following domain: $x_0 \le x \le x_k$, $0 \le z \le z_k$, where $x >> z$, $x >> \Delta x$, with $\Delta x = x_k - x_0$.

Under these conditions we obtain

$$v \approx x^m \psi(z/x).$$

As variations in the value of x are relatively small inside this limited domain, we can write

$$x_k = x_0(1 + \Delta x/x_0) \approx x_0, \text{so } \psi(z/x) \approx g(z) \text{ or } v \approx x^m g(z).$$

Thus inside the chosen domain the two velocity functions have a close resemblance. If we substitute $m = 0$, then obviously within the domain the homogeneous function is effectively a function of depth, i.e. $v(x,z) \approx g(z)$. Thus a 1D inhomogeneous model is the limiting case of a zero-degree homogeneous function. As we never use a velocity function in a whole, infinite half-plane, the assumptions do not limit the generality of this conclusion. Thus a simple horizontally layered medium with constant velocities V_1, V_2, V_3, ... and interfaces Z_1, Z_2, Z_3, ... can be approximated by a zero-degree homogeneous function as closely as desired, although the arbitrary function of depth is not a homogeneous function.

We note that the class of homogeneous functions is wider than the class of functions $x^m f(z)$, because the homogeneous functions can describe seismic media with boundaries of arbitrary inclination including those that are effectively horizontal, but the functions $x^m f(z)$ can describe only media with horizontal boundaries.

Thus homogeneous functions can describe layered media with linear seismic boundaries, waveguides and folded zones. Using homogeneous functions for a local approximation, we can describe an arbitrary velocity distribution.

PROPERTIES OF TRAVELTIME CURVES FOR MEDIA WHERE VELOCITY IS A HOMOGENEOUS FUNCTION

The following important properties of traveltime curves are used for solving the inverse problem. The traveltime curves (of direct, head, diving and reflected waves and also the first arrivals of the waves) obtained from different sources at the surface of a medium with a homogeneous velocity function are similar to each other. All the equations below hold for any two traveltime curves of the same type.

We use polar coordinates to describe the traveltime curves.

1 For any two traveltime curves $t_1(r_1)$ and $t_2(r_2)$ of the same type with sources at the points r_{01} and r_{02} on the surface $\varphi = 0$ of medium 1, we can write

$$\frac{r_1}{r_2} = \frac{r_{01}}{r_{02}} \Rightarrow \frac{t_1}{t_2} = \left(\frac{r_{01}}{r_{02}}\right)^{1-m}, \tag{2}$$

where m is the degree of the homogeneous function (1). With knowledge of any one traveltime curve from a source on the surface of medium 1, the traveltime curve from a source at any other point on the surface of medium 1 can be calculated using a linear transformation.

2 For two reverse traveltime curves $t_1(r_1)$ and $t_2(r_2)$ in the interval $[r_{01},r_{02}]$ on the surface $\varphi = 0$ of medium 1, with sources at the points r_{01} and r_{02}, we can write

$$r_1 \cdot r_2 = r_{01} \cdot r_{02} \Rightarrow \left(\frac{t_1}{t_2}\right) = \left(\frac{r_{02}}{r_1}\right)^{1-m}. \tag{3}$$

This transformation maps a forward traveltime curve on to an inverse one and vice versa.

Function (1) can include velocity discontinuities and intervals where there is a minimum. Accordingly, seismic media with velocity 1 can contain boundaries and waveguides. Traveltime curves at the surface of media 1, can, in turn, be multivalued and include shadow zones. Traveltime curves of head and reflected waves can also be present. All these singularities agree with the results of transformations (2) and (3). Thus we can identify automatically waves from different layers on the reverse traveltime curves of first arrivals. This is a common problem, which is difficult to solve.

Furthermore, traveltime curves for medium 1 possess important properties. The media under investigation are two-dimensionally inhomogeneous. There is no limit on the horizontal component of the velocity gradient. However, traveltime curves for medium 1 can be converted to traveltime curves corresponding to a 1D medium whose velocity depends only on the polar angle. Let $t(r)$ be a traveltime curve with source at the point r_0 on the surface of medium 1. Then the transformations,

$$\rho = r^{1-m},$$
$$\rho_0 = r_0^{1-m}, \tag{4}$$
$$\tau = |1 - m|t,$$

will convert $t(r)$ to traveltime curve $\tau(\rho)$ with source at ρ_0 for a medium with velocity $\xi = \xi(\alpha)$, where

$$\alpha = |1 - m|\varphi, \quad \xi = \psi. \tag{5}$$

More details are given in the Appendix.

Transformation (4) enables us to convert forward and inverse problems for medium 1 into 1D cases. This property is used for solving the inverse problem.

INVERSE PROBLEM

The homogeneous velocity function (1) can be calculated using two reverse traveltime curves of first arrivals. Let the Cartesian coordinates (x,z) define a point in some 2D medium and let $t_1(x_1)$ and $t_2(x_2)$ be two reverse traveltime curves at the surface $z = 0$ of the medium. The coordinates of the sources are x_{01} and x_{02} and points on the traveltime curves are defined in the interval $[x_{01},x_{02}]$. We search for a best approximation of the unknown velocity distribution in the medium by a homogeneous function in two coordinates. We assume that the origin of the local polar coordinates is at the point $x = c$ on the surface $z = 0$, where c can be either to the right or to the left of the interval $[x_{01},x_{02}]$. Then the radial coordinates of points on the profile are $r = | x + c |$ and the unknown velocity function, in Cartesian coordinates, has the form,

$$v = \left(\sqrt{(x + c)^2 + z^2}\right)^m \psi\left(\arctan\left(\frac{z}{|x + c|}\right)\right), \tag{6}$$

where m, c and the values of the function ψ are unknown parameters. Initially, arbitrary values are assigned to the parameters m and c. Equation (3), which in Cartesian coordinates can be written in the form,

$$x_2 = \frac{(x_{01} + c)(x_{02} + c)}{x_1 + c} - c, \quad t_2 = \left(\frac{(x_{02} + c)}{(x_1 + c)}\right)^{1-m} t_1, \tag{7}$$

is then used to convert the given inverse traveltime curve $t_2(x_2)$ into a forward one. The traveltime curve $t_1^s(x_1)$ thus obtained may differ from the given forward traveltime curve $t_1(x_1)$. The mean square deviation between the given forward traveltime curve $t_1(x_1)$ and the transformed traveltime curve $t_1^s(x_1)$ is a function of the two variables m and c: $f(m,c)$. Let the coordinates of the minimum point of $f(m,c)$ be m^* and c^*, so that

$$f(m^*, c^*) = \min f(m, c) = f^*.$$

These parameters m^* and c^* give the homogeneous function that is the best approximation of the real velocity distribution. The value of f at the minimum point is f^* and it defines the error of the approximation. The function $f(m,c)$ is minimized using standard algorithms for minimizing a function of several variables. We note that at each step in the evaluation of $f(m,c)$ we do not calculate seismic rays as is done in ray-tracing algorithms, but instead we perform simple transformations of a reverse traveltime curve into a forward traveltime curve. Since homogeneous functions are infinite-dimensional functions, they provide good approximations, with errors that are always close to the time uncertainties for a given experiment, as numerous tests and investigations have shown.

Knowing the location of the polar origin (parameter c), we can now use polar coordinates. The reverse traveltime curve $t_2(r_2)$ can be transformed into the forward traveltime curve $t_1^s(r_1)$ using (3) and m^* and c^*. The deviation between $t_1(r_1)$ and $t_1^s(r_1)$ is now a minimum. Next we calculate the average traveltime curve,

$$\bar{t}(r_1) = 1/2(t_1(r_1) + t_1^s(r_1)).$$

We assume that the traveltime curves $\bar{t}(r_1)$ with source at the point r_{01} correspond exactly to the required homogeneous function with parameters m^* and c^*. It is now necessary to find values of the function $\psi(\varphi)$ from (6). We use the property of traveltime curves, discussed above, that enables conversion of the traveltime curves into those for 1D media. Applying transformation (4) to $\bar{t}(r_1)$, we obtain the traveltime curve $\tau(\rho)$ with source ρ_{01} corresponding to an unknown velocity $\xi = \xi(\alpha)$. The function $\xi = \xi(\alpha)$ can include breakpoints and intervals where it has minimum values. In order to obtain velocity boundaries in the cross-section, we represent the function $\xi = \xi(\alpha)$ as a step function,

$$\{\xi = \xi_i = \text{const}, \quad \alpha_i \le \alpha \le \alpha_{i+1}\}_{i=0}^{i=n}, \quad \text{for } \{\xi_{i+1} > \xi_i\}_{i=0}^{n}, \tag{8}$$

where n is the number of points of interpolation on the traveltime curve $\tau(\rho)$ (we use $n = 90$). In media with velocity given by (8) head waves exist and the traveltime curve of the first arrivals consists of linear intervals. We now represent $\tau(\rho)$ as a broken line with n intervals. It is necessary to calculate ξ_i and $\Delta\alpha_i = \alpha_{i+1} - \alpha_i$ from the traveltime curve $\tau(\rho)$. This problem is solved using a known formula for head-wave kinematics (see Appendix). At the same time the set of seismic rays with source at ρ_{01} is calculated. However, in addition we must assume that the values ξ_i increase with increasing α_i, as is required by the kinematics of head waves. Thus we have defined an increasing function $\xi = \xi(\alpha)$ and consequently function (6) has been determined completely. The calculated homogeneous function approximates the real velocity distribution only in the area where the seismic rays corresponding to a given pair of reverse traveltime curves penetrate. To define this area we use the last ray from a set of rays calculated in the process of finding the function $\xi = \xi(\alpha)$, and calculate the ray that passes through the sources r_{01} and r_{02}. We call this ray the boundary ray. The region defined by the boundary ray and the area of surface with known velocity function is called the local velocity field. For a complex set of observed traveltime curves, the final velocity cross-section is constructed from the local velocity fields.

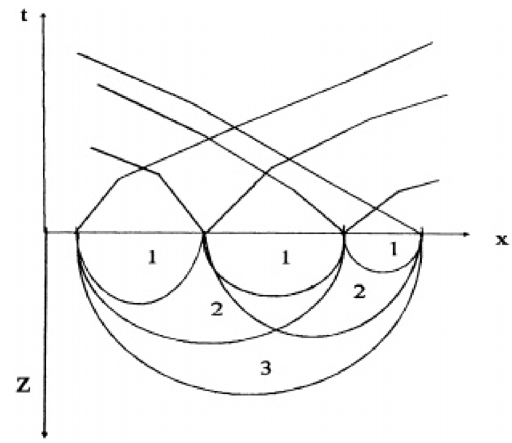

Figure 2 Construction of the final cross-section from local velocity fields using the priority system. The traveltime curves and the plan of the cross-section including the boundary rays of the local velocity fields are shown. Values of priority are indicated by the numbers 1, 2 and 3.

CONSTRUCTION OF FINAL VELOCITY CROSS-SECTION

The final cross-section is constructed by a method of superposition of the local velocity fields. Assume a system of observation as shown in Fig. 2. One possible approach is as follows. The local velocity field is calculated for every pair of reverse traveltime curves chosen from the system of traveltime curves. First the local velocity fields for the shortest pairs of reverse traveltime curves, denoted in Fig. 2 as 1, are calculated (a 'short pair' of traveltime curve means a short distance between the sources corresponding to the pair of reverse traveltime curves). Then the velocity distribution is known for depths less than or equal to h_1, where $h_1 = \min(h_i)$ and h_i are the depths of maximum penetration of rays for the shortest pairs of traveltime curves. Next, the observed traveltime curves are recomputed at the first level h_1, i.e. the downward continuations of the first arrivals at this level are constructed, and then the process of calculations is repeated. It is not a difficult technical problem. However, the calculated velocity distribution in the first band is an approximation and differs from the real velocity distribution. Consequently in the process of the recomputation of traveltimes, errors accumulate. In addition the process is too complex.

However, here we use a different approach. Suppose that we can calculate an arbitrary velocity function of two coordinates using the data of two reverse traveltime curves. Then the local velocity field calculated for the longest pair of reverse traveltime curves would coincide with the local velocity field for any of the shorter pairs of traveltime curves at all points where they cover the same subsurface area. However, the homogeneous function (1) is not an arbitrary function of two coordinates (r,φ) or equivalently (x,z). It changes as an arbitrary function in the subvertical direction, but it also changes as a power function in the subhorizontal direction. In this case the approximation is better if the shot distance of the reverse pair is shorter. Therefore, the local velocity field corresponding to a shorter pair of traveltime curves is a better approximation of the real velocity distribution and we replace the local values of velocity corresponding to longer shot distances with values of the shorter shot distance at those points where they cover the same subsurface area.

Thus, we construct a final seismic cross-section using a system of priorities. Let the traveltime curve system consist of several pairs of reverse traveltime curves (Fig. 2). Then the local velocity fields corresponding to the shortest distance between shotpoints, denoted by 1, receive the highest priority. Velocity values corresponding to these local velocity fields are always present in the cross-section. Velocity values of local velocity fields, corresponding to pairs of traveltime curves with greater distance between shotpoints (denoted by 2 and 3), are present in the velocity cross-section when a velocity point corresponding to a shorter traveltime curve is absent. At the points of intersection of local velocity fields with the same priority, the average velocity value is calculated. Thus, only the lower parts of the local velocity fields determined by the longer distance between shotpoints are present in the cross-section (Fig. 2).

Every local velocity field is defined by its own homogeneous velocity function, i.e. the values of m, c and $\psi(\varphi)$ vary for different local velocity fields. These values are calculated independently, from different pairs of the reverse traveltime curves. In order to calculate the approximate homogeneous functions we use the formula for kinematics of head waves; consequently the following limitations characterize the local velocity functions. The functions $\psi(\varphi)$ increase with polar angle. Waveguides can be present on the final cross-section only on the boundaries between different local velocity fields. The velocity inside the waveguides is defined as an effective-velocity function. The hidden layer problem also occurs. In this case an effective-velocity distribution is obtained in the blind zone.

It has been shown (Piip and Efimova 1987) that the algorithm is stable. Velocity values corresponding to different local velocity fields overlap significantly in the final cross-section, and boundaries of local velocity fields are not apparent in the final velocity field. In general, the local velocity fields computed for neighbouring pairs of traveltime curves are virtually coincident at their points of intersection. The error in velocity computation may be defined by the difference in velocity values at these points. Occasionally, but in not more than 5% of cases, the local velocity field differs significantly from a neighbouring local velocity field. In such a case, the boundaries of the local velocity field are seen in the common cross-section, drawn as a contour field with equal intervals. Such local fields must be eliminated from the cross-section. In this case the velocity values are replaced automatically by values of the local velocity field with a lower priority.

Numerous tests of cross-sections calculated by these methods show that they fit the data within generally accepted limits (Piip and Efimova 1985, 1990, 1996, and examples in this paper).

We note here that analogous methods of construction of cross-sections using the approximation of overlapping layers by an effective constant velocity (for example, the plus–minus method) are applied widely in refraction and reflection seismic exploration.

THEORY STATEMENTS

Mathematical proofs of the following statements are given in the Appendix.

1 Traveltime curves recorded at the surface of a medium with a homogeneous velocity function, and sets of rays and wavefronts whose sources lie on the same radial line are similar. This is true for both refracted and reflected waves. For two reverse traveltime curves, non-linear continuous transformations exist which continuously map the forward traveltime curve on to the reverse one and vice versa. These transformations have enabled us to develop an automatic procedure of identification of waves refracted at different seismic boundaries for the reverse traveltime curves of first arrivals.

2 The differential equation of a ray for a medium with a homogeneous velocity function is a first-order equation. The seismic ray has a constant parameter along its path.

3 Homogeneous functions of two coordinates describe a medium whose velocity depends essentially on two coordinates. However, the rays and time fields corresponding to these velocity functions can be transformed to those for a medium whose velocity depends on one coordinate only, i.e. the polar angle. This is illustrated in Fig. 1, where the rays and time fields corresponding to the media shown in columns 2 and 3 can be transformed into those for the media shown in the first column.

4 These properties of homogeneous velocity functions have enabled us to solve the inverse kinematic problem for such media, i.e. to reconstruct the velocity field using the data of a pair of reverse traveltime curves of refracted first arrivals. A system of curved seismic rays is computed in the course of solving the problem. The algorithm for the solution of this inversion problem is stable (Piip and Efimova 1987). Thus in the case of a complex shooting geometry, the common-velocity cross-section may be constructed by application of a local approximation of the real velocity distribution using homogeneous functions. In general, the acquisition system includes a few pairs of reverse traveltime curves and therefore the final cross-section is constructed using the method of superposition of local velocity fields, corresponding to different pairs of reverse traveltime curves.

THE GODOGRAF PROGRAM

The theory stated above has served as the basis for the creation of a computer program known as GODOGRAF. It has provided the following results.

1 Complete automation of the interpretation process. First-arrival traveltime curves are used only as data. An initial model is not needed for the inversion process. It is not necessary initially to distinguish between the refracted waves from different refracting boundaries and to identify them on the traveltime curves. This is performed automatically.

2 A continuous velocity cross-section is obtained, where the velocity and its gradient are known for every point. The seismic boundaries in such a cross-section are of two types. In the first type, the boundaries are lines where the velocity is discontinuous and in the second type, the boundaries are lines where the velocity gradient is discontinuous.

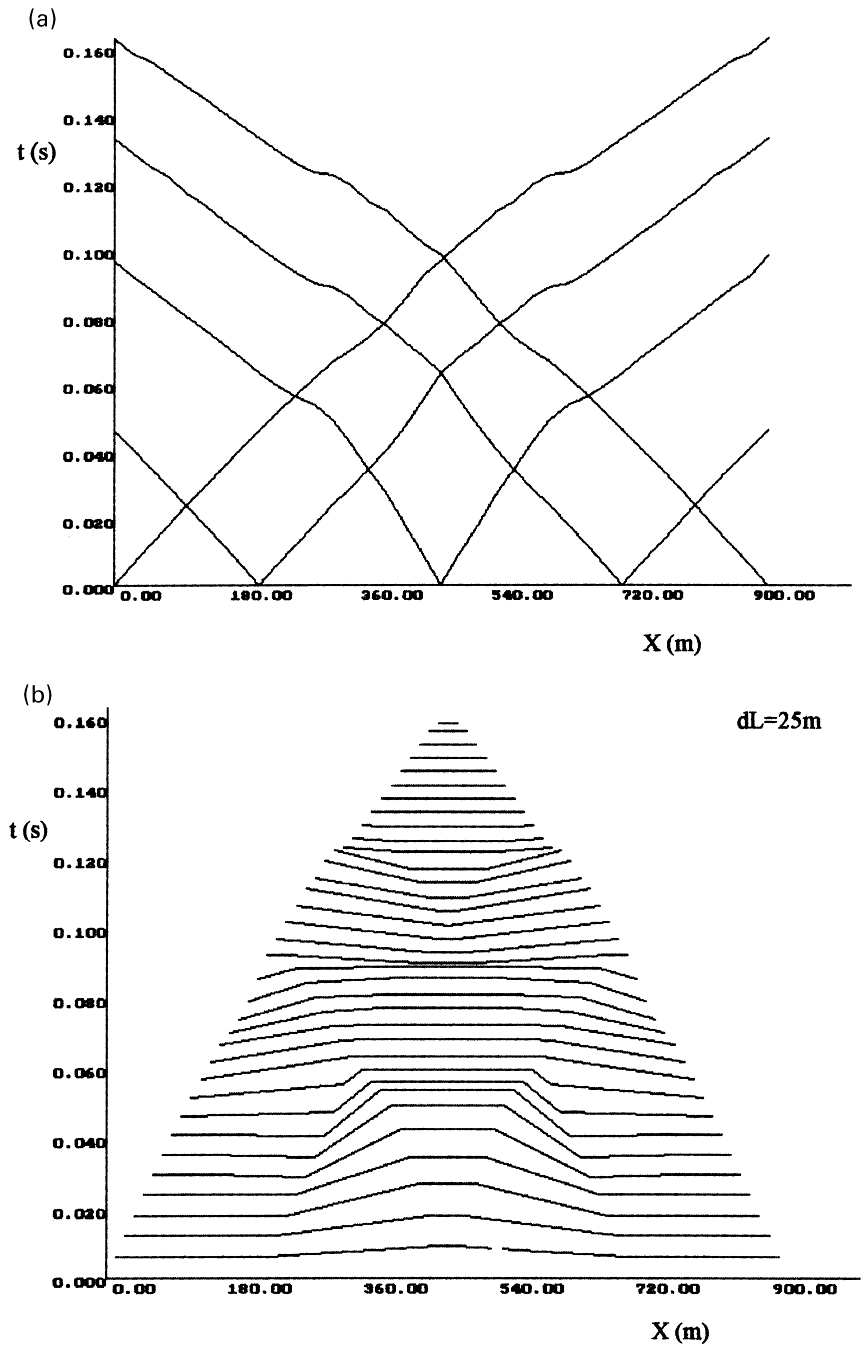

Figure 3 (a) Refraction traveltime curves computed for the trough model; (b) the time field $t(x,L)$ corresponding to refraction traveltime curves. In (a) the traveltime curves $x_0(x_1,t)$ represent the contours $x_0 = \text{const}$ (x_0 is the abscissa of the shotpoint, x_1 is that of the receiver); (b) time field $t(x,L)$ shows the same traveltime curves but with the coordinates $x = (x_0 + x_1)/2$, $L = \text{abs}(x_0 - x_1)$. The contours $L = \text{const}$ are drawn at equal intervals of 25 m. It can be seen that the time field $t(x,L)$ maps the main features of the model.

3 A geological interpretation of the seismic cross-section is made by the interpreter. The different layers, boundaries and faults are identified. The seismic cross-section is a velocity field defined by velocity values calculated at the nodes of a 250×100 rectangular grid. The velocity contours are drawn at equal intervals and the values of the velocity and velocity gradient can be evaluated visually at every point on the cross-section. The boundaries, folds and faults are mapped on the velocity fields and can be traced by the interpreter. Each layer has an inner structure, characterized by dominant values of the velocity gradient and its own contour pattern.

4 Horizontal velocity map-slices are constructed at different depths, if there are several refraction profiles in the area under investigation. Representing a cross-section as the

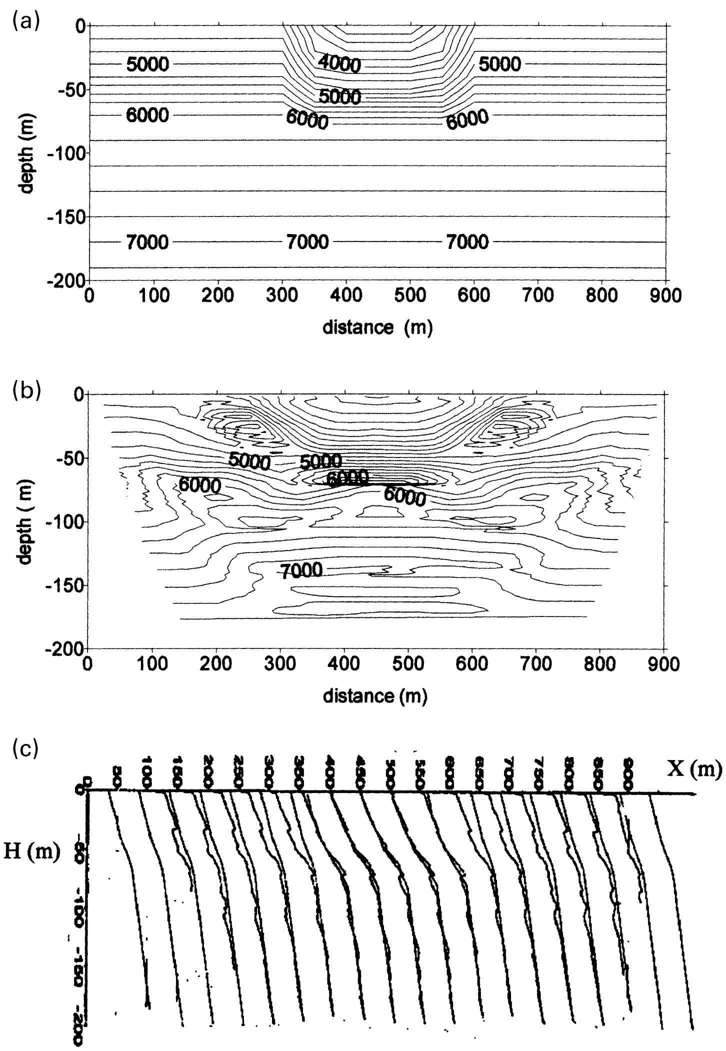

Figure 4 Comparison of the velocity fields for the trough model: (a) the given field; (b) the result of inversion; (c) a comparison of the given (smooth) and the restored vertical velocity functions for the same model. The contour interval is 200 m/s. The vertical magnification is 2:1.

velocity field given at the nodes of a rectangular grid enables easy interpolation. It is possible to calculate horizontal velocity map-slices and to construct 3D structures.

5 The system of traveltime curves can be interpolated. It is also possible to compare the structures on the cross-sections obtained with the corresponding features on the traveltime curves. We represent the refraction traveltime curves of the first arrivals by the coordinates (x,L) and construct the time field $t(x,L)$. Here, x is the coordinate of the centre of a base (a base being the interval between a source and a receiver) and L is the length of a base. The contours $L = \text{const}$ are drawn in the time field $t(x,L)$ at equal intervals. This time field is analogous to a time-section for reflected waves obtained by the common-midpoint method. The main features of a cross-section at depth are revealed in such a time field. This method for imaging of traveltime curves was proposed by Puzyrev (1963).

GODOGRAF is a universal program for the interpretation of any system of refraction traveltime curves obtained by any refraction method. It can be used in both shallow seismic and deep investigations of the crust and mantle, including engineering, exploration for oil and deep seismic sounding. The minimum shooting geometry required to apply this inversion method is two shotpoints. The high accuracy of the velocity computation enables the velocity field contours representing the cross-sections to be constructed at small intervals, usually from 0.02 km/s to 0.2 km/s. The seismic boundaries are seen as lines of high-density velocity contours or lines where the density of contours changes sharply.

Examination by ray tracing of the cross-sections computed with this method has shown that observed and calculated times are consistent (Piip and Efimova 1985, 1990, 1996, and the example in this paper). This inversion method is now used

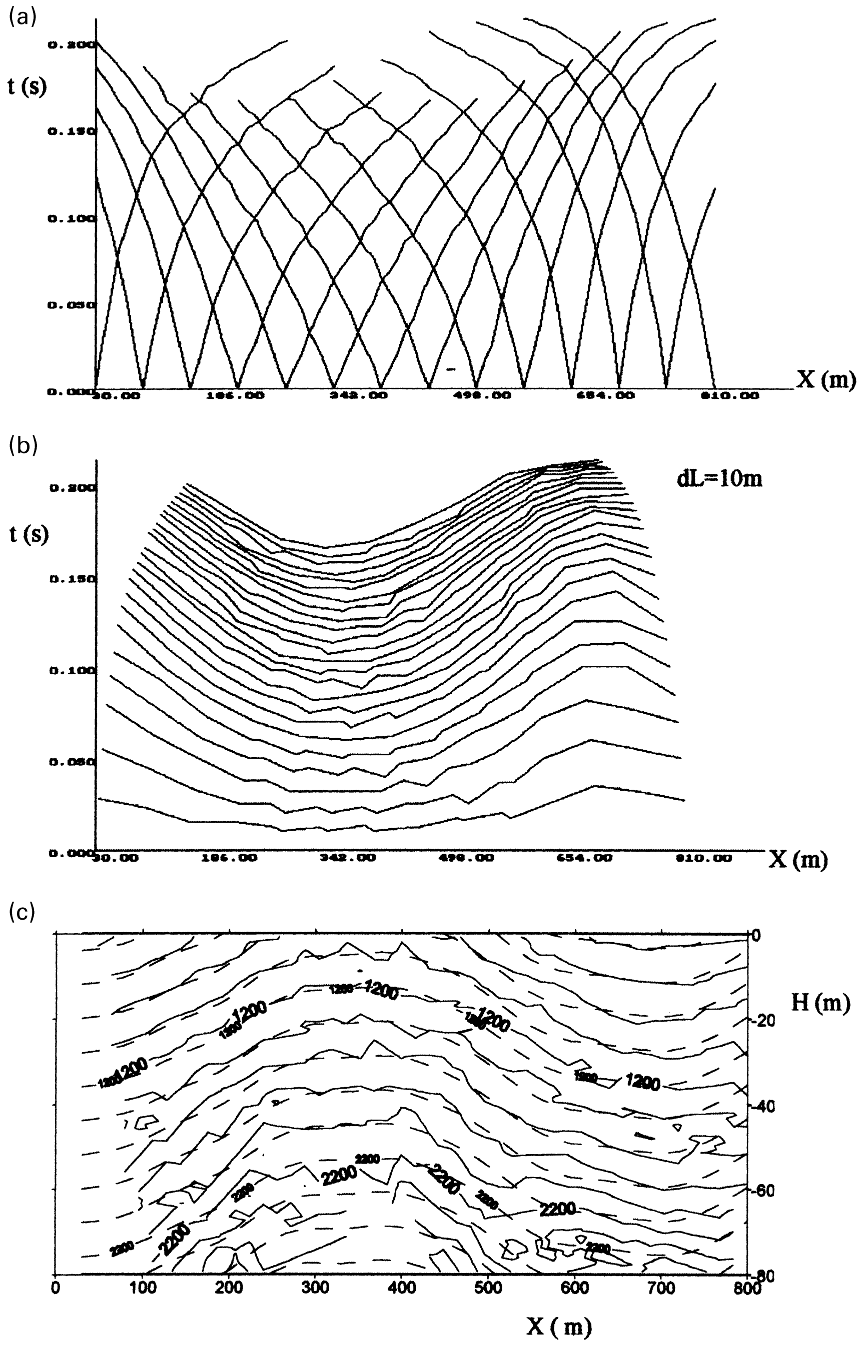

Figure 5 Inversion of traveltime curves for a model with sine-shaped velocity contours: (a) the computed traveltime curves with an error of approximately 1%; (b) the time field $t(x,L)$ corresponding to the traveltime curves; (c) a comparison of the given contours (dashed lines) with the inversion contours (continuous lines). The contour interval is 200 m/s. The vertical magnification is 4:1.

in Russia for investigating shallow depths in engineering seismic and for interpreting deep seismic sounding data.

NUMERICAL SIMULATION

The potential of this inversion method has been investigated by numerical simulation (Piip 1978, 1982a,b, 1984). We now consider two models. The traveltime curves $t(x,x_0)$ for the first trough model are shown in Fig. 3(a). This is a generally accepted method of imaging traveltime curves where the contours x_0 = const are drawn. In this case, x denotes the abscissa of the receiver and x_0 denotes the abscissa of the source. The model (Fig. 4a) is composed of two horizontal layers where the vertical velocity gradient is present. The layers are divided by a transient layer with an increased gradient value. In the upper layer, the trough is represented by a domain with low velocity values. Two vertical transient zones separate the trough from the embedding layer. The time field $t(x,L)$ is shown in Fig. 3(b). This is another representation of the traveltime curves where the contours $L = | x - x_0 | =$ constant, with $dL = 0.25$ m, are drawn. It can be seen that the main features of the model are represented in the time field. The model obtained as the result of the inversion is shown in Fig. 4(b). All the structures of the given model are present in the cross-section obtained. In the central part of the model the velocity values, velocity gradient values and depths are recovered well at all depths of ray penetration. This can be seen in Fig. 4(c), where sets of vertical velocity functions, both given and computed, are compared. The model was piecewise recovered, demonstrating the high stability of the algorithm. However, significant errors are present in the upper edges of the model. These can be explained by the low density of penetrating rays here.

The traveltime curves computed for a second model with sine-shaped velocity contours are shown in Fig. 5(a). Approximately 1% noise with rms deviation of 0.002 s was added to the computed time values. The time field $t(x,L)$ (see Fig. 5b) images the structure of the velocity contours. The recovered model obtained using GODOGRAF is shown in Fig. 5(c), where the given velocity contours are represented by dashed lines. They appear as an average of the reconstructed velocity contours. Forty-six local velocity fields were used for constructing the final cross-section.

FIELD EXAMPLE 1: REFRACTION INVESTIGATION INTO THE SALAIR MULTIMETALLIC DEPOSIT

High and variable values of the velocity gradient are usual for seismic cross-sections in ore deposit regions. The interpretation of refraction traveltime curves is very difficult using traditional methods. This example illustrates the potential of the refraction inversion technique using a local approximation of real velocity fields by homogeneous functions.

The seismic profile is located at the northeast of the Salair deposit, which contains multimetallic ores. The deposit is situated on the slope of a large anticline, near the junction of the Salair ridge and the Kuznetskaya trough (South Siberia, Russia). The ore field is an oval lens of magmatic and metamorphosed rocks, embedded in limestone. The area is enriched by metals and barite formed above intrusive bodies along transverse faults. Chemical and physical weathering crusts and karst troughs have developed there.

The Central Geophysical Expedition (Novokuznetsk, Russia) carried out the seismic work. The profile length is 750 m. Many wells were drilled along the profile. Fourteen of the wells were terminated at the limestone top. Two wells reached the karst trough bottom. Four wells passed the whole seismic cross-section depth near the karst trough.

The refraction traveltime curves (Fig. 6) have a complex form. The time field $t(x,L)$ for the Salair profile is shown in

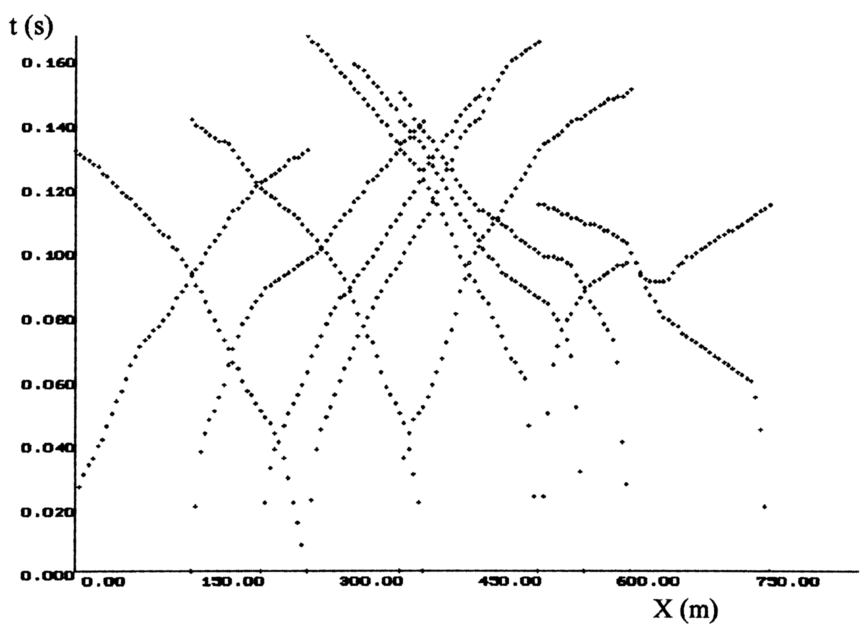

Figure 6 Refraction traveltime curves along the profile in the Salair deposit region.

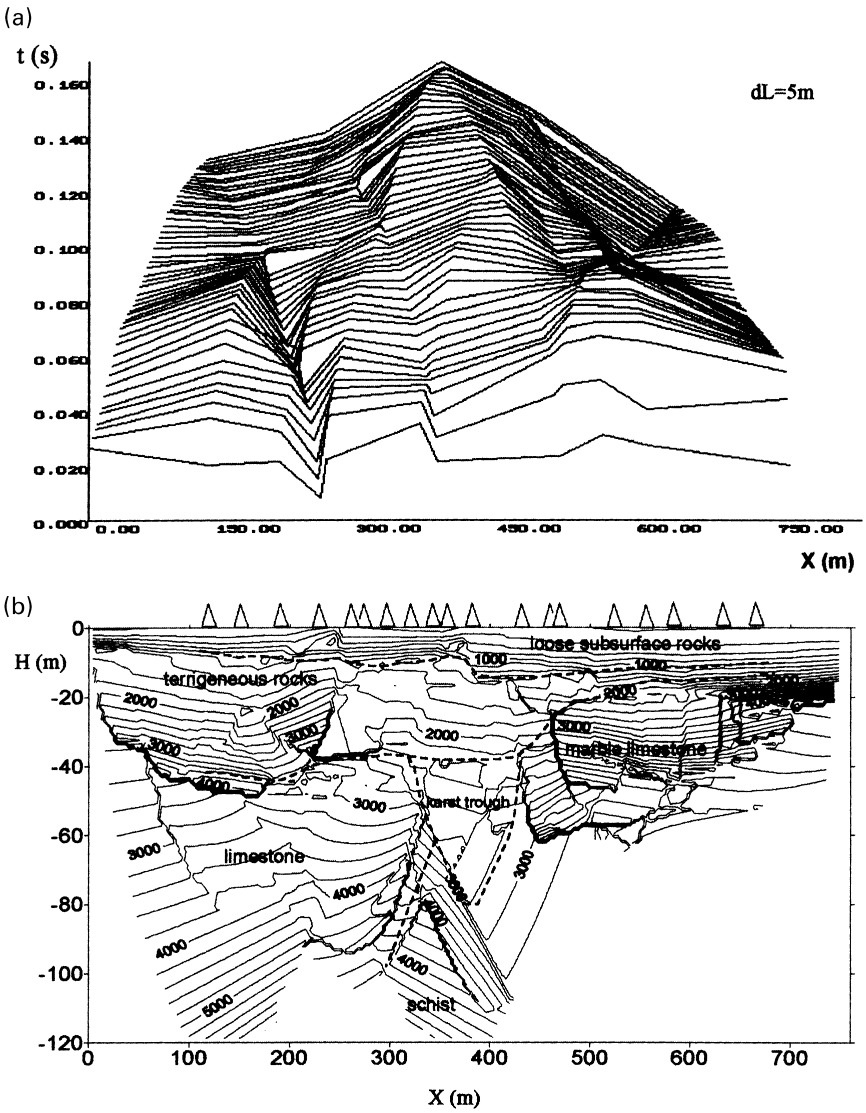

Figure 7 (a) Refraction time field $t(x,L)$ for the Salair profile; (b) the velocity seismic cross-section as a result of inversion. The positions of wells are shown on the surface. The dashed lines indicate the lithological boundaries obtained from the well data. The contour interval is 200 m/s. The vertical magnification is 4:1.

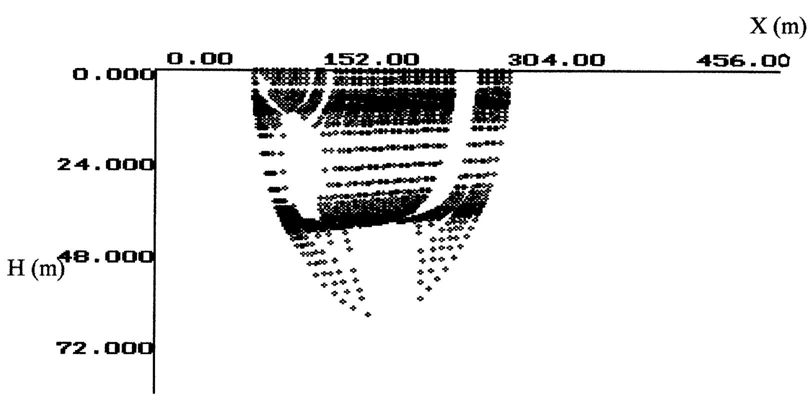

Figure 8 The ray diagram computed with the inversion process for the 80–310 m interval on the Salair profile. The points of intersection of rays and the ϕ = const levels are shown here. The main refraction boundaries are visible, because the seismic rays are focused near boundaries.

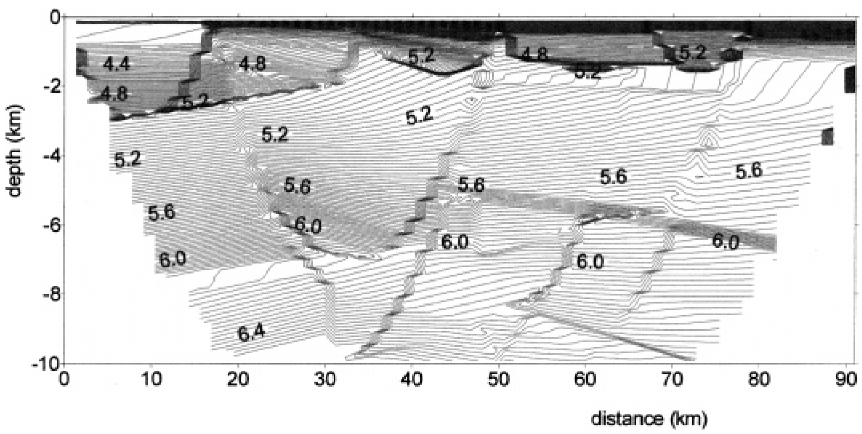

Figure 9 Seismic cross-section along a profile located in the central part of the Moscow region. Only the velocity contours are shown in the cross-section. The contour interval is 0.02 km/s. The top of the crystalline basement is seen at a depth of 6–7 km as a boundary of the first type in the right-hand part of the cross-section and as a boundary of the second type in the left-hand part of the cross-section. The vertical magnification is 4:1.

Fig. 7(a), where a deep trough is visible near the 350–400 m interval of the profile. The positions of the wells are shown in Fig. 7(b), where a seismic cross-section obtained as a result of the inversion is represented by velocity contour lines. Dashed lines represent the lithological boundaries based on the borehole data. The velocity contour lines are drawn at equal intervals (200 m/s) on the cross-section. The layers and structures contained in the cross-section are (from top to bottom): loose subsurface rocks, terrigenous rocks, limestone, marble limestone, karst trough and schist. The disturbed schist includes the orebodies. Figure 7(b) shows good correlation between the seismic cross-section and the well data.

A set of seismic ray curves is calculated during the solution process. For example, the ray diagrams for the Salair cross-section are shown in Fig. 8. Refraction rays calculated for the 80–310 m interval of the profile are represented here by the points of intersection of rays and the φ = const levels. The main refracting boundaries are visible in this figure because the seismic rays are focused near seismic boundaries.

FIELD EXAMPLE 2: INVESTIGATION INTO THE BASEMENT STRUCTURE IN THE MOSCOW REGION

GODOGRAF was used to reinterpret previous refraction data obtained in order to investigate the crystalline basement structure in platform regions. It is known that the cross-section obtained using the common-midpoint reflection method does not reveal the inner structure of the basement sufficiently well. Reinterpretation of the previous refraction data obtained along profiles located in the Moscow region has shown that significant complementary information may be gained using the homogeneous function method. The acquisition geometry includes 5–7 shotpoints for every profile of 150–200 km length, i.e. the shotpoint spacing is approximately 30 km. The length of the traveltime curves achieved is 70 km and the distance between the receivers is 100 m. The top and interior structure of the basement are sufficiently clear in the new cross-sections. Figure 9 shows the cross-section along profile V-63. This profile is located in the eastern part of the investigated area and the basement structure can be clearly seen here. The top of the crystalline basement can be seen on the right-hand side of the cross-section represented by a sharp boundary of the first type or a narrow transient zone, where velocity values increase from between 5.6 and 5.7 km/s to between 5.8 and 6.0 km/s. On the left-hand side of the cross-section, the top of the basement is seen as a boundary of the second type. Most faults are represented here by boundaries of the first type but not all of them can be traced in the upper layer.

FIELD EXAMPLE 3: SEISMIC CROSS-SECTION OF THE EARTH UNDER THE KLUCHEVSKAYA VOLCANIC GROUP

The homogeneous function method of refraction inversion may be used in very complex geological conditions for imaging of deep regions of the earth's crust.

The seismic surveys in Kamchatka (Russia) were carried out by the Institute of Volcanology (Russian Academy of Sciences) in 1986–7 along a profile 60 km in length that crossed the central part of the Kluchevskaya volcanic group (Fig. 10) (Balesta *et al.* 1992). The detailed system of the refraction traveltime curves (Fig. 10a) was reinterpreted

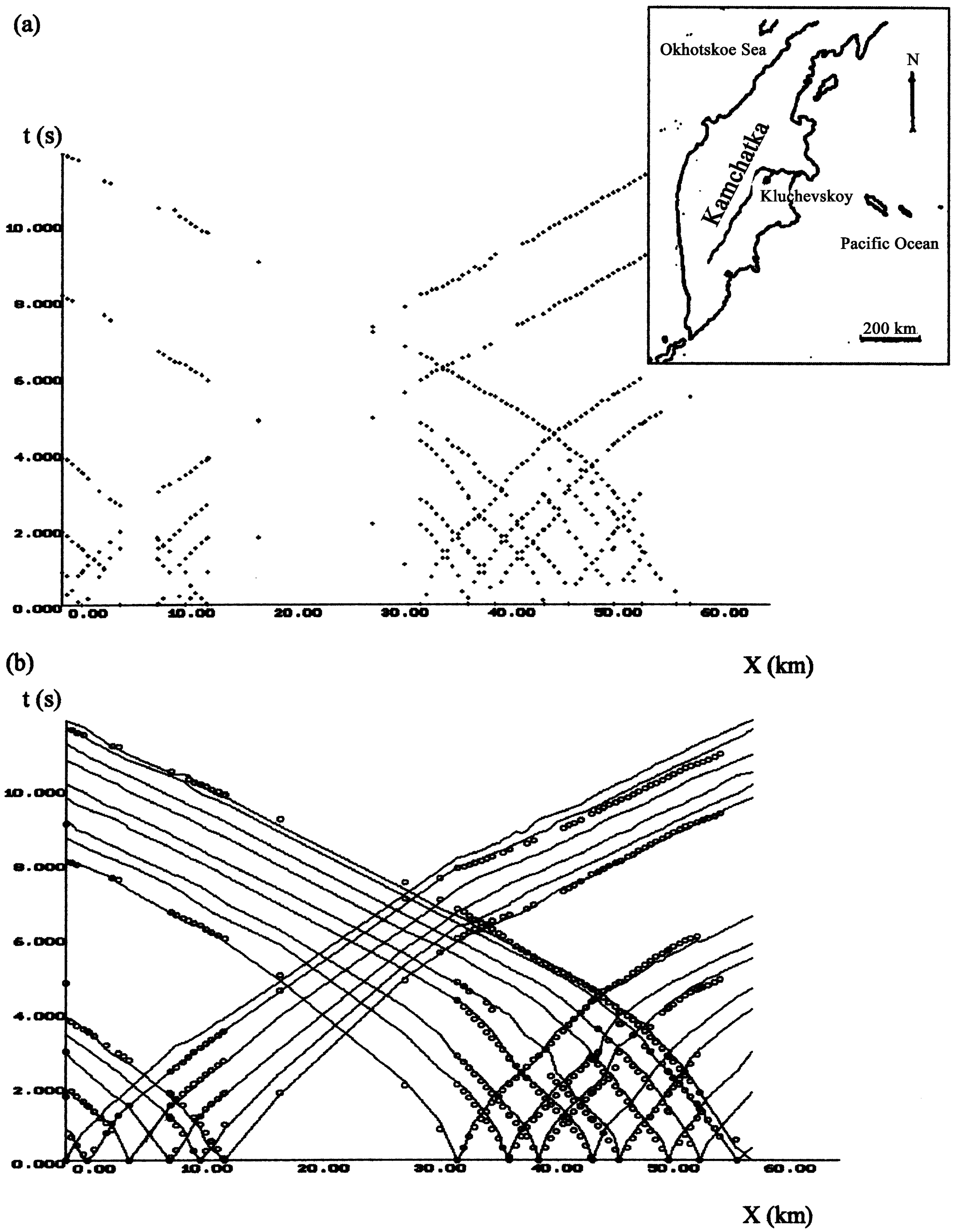

Figure 10 (a) The traveltime curves along a profile through the Kluchevskoy volcano (Kamchatka, Russia). The inset shows the location of the volcano. (b) The interpolated observed traveltime curves used for inversion (thin lines) and the times (circles) calculated by two-point ray tracing.

using the homogeneous function technique. Figure 10(b) shows the interpolated traveltime curves. These were used for the inversion. The final cross-section is composed of 109 local velocity fields. The final cross-section was obtained automatically and then its geological interpretation was added manually (Fig. 11).

Several subparallel layers can be traced in the cross-section. From bottom to top these are: the crystalline basement denoted by B in Fig. 11 (the velocity values near the top are 5.5–6.2 km/s and the velocity gradient is nearly constant at approximately 0.25 1/s); an upper Cretaceous basement denoted by K2 (velocity interval of 5.3–5.8 km/s); a Palaeogene layer denoted by P (velocity interval of 4.2–5.3 km/s). Quaternary and Neogene layers lie above. All these layers are divided into blocks by many listric and linear faults. The main low-angle (45°) thrust listric fault is located directly under the volcanoes. A sharp, restricted domain with reduced velocity is present in the crystalline basement at a depth of about 8 km, where the listric fault terminates. This domain is interpreted as the magma chamber. Other anomalies are also present along this fault.

The cross-section was verified by solving the direct problem with two-point ray tracing (Ditmar and Roslov's FIRSTOMO computer program was used). The calculated times agree with the observed ones sufficiently well as is shown in Fig. 10(b). The mean square deviation of the calculated times from the observed ones is 0.12 s.

CONCLUSIONS

1 The homogeneous function method produces an automatic 2D inhomogeneous simple inversion of refraction traveltime curves for first arrivals. It does not require an initial model, and preliminary distinguishing and identification of waves on the traveltime curves are unnecessary.

2 Velocity cross-sections calculated by the homogeneous function method fit the traveltime curves sufficiently well.

3 The homogeneous function method may be used for inversion of any refraction profile data, obtained from both shallow and deep seismic methods.

4 The homogeneous function method affords the imaging of very different and complex geological media including the boundaries of layers, faults, folded zones and velocity anomalies.

ACKNOWLEDGEMENTS

The author thanks Dr P.M. Bakker and Dr P.H.A. Gerritsma for their reviews and constructive comments on this paper. The author is also grateful to Professor T.I. Oblogina and Dr E.A. Efimova for cooperation.

REFERENCES

Adachi R. 1954. On a proof of a fundamental formula, concerning the refraction method of geophysical prospecting and some remarks. *Kumamoto J. Science, Seria A* **2**, 18–29.

Balesta S.T., Gontovaya L.I., Kargopoltsev A.A., Pak G., Pushkarev V.G. and Senyukov S.L. 1992. Results of seismic studies of the earth crust in the region of the Kluchevskoy volcano. *Volcanology and Seismology* **13**, 269–286.

Boldyrev S.A., Kaz S.A. and Ponomarev S.F. 1982. Algorithms and method of studying 3D velocity nonhomogeneities from kinematic residuals on an example of mantle block of the Sea of Okhotsk. In: *Application of Numerical Methods in Investigation of the Lithosphere* (ed. A.S. Alekseev), pp. 29–42. Academy of Sciences, USSR (in Russian).

Červený V., Molotkov I. and Pšenčík I. 1977. *Ray Methods in Seismology.* University of Karlova, Prague.

Ehrenfest-Afanassjewa T. 1915. Der Demencionsbegiriff und der analytische Bau physikalischer Gleichungen. *Mathematische Annalen* **LXXVII**(2), 28–45.

Ganzha O.Yu. 1982. Solving of inverse kinematic problem of seismic prospecting by the method of optimisation. In: *Application of Numerical Methods in Investigation of the Lithosphere* (ed. A.S. Alekseev), pp. 66–74. Academy of Sciences, USSR (in Russian).

Piip V.B. 1978. The method of definition of cross-section of the velocity contours on the data of refraction traveltime curves. *Fizika Zemli* **8**, 65–72 (in Russian).

Piip V.B. 1982a. The use of homogeneous functions for approximation of seismic velocity cross-section. *Izvestiya, Academy of Sciences, USSR, Physics of Solid Earth* **17**, 540–546.

Piip V.B. 1982b. Simplified method of construction of seismic cross-section with velocity contours. *Applied Geophysics* **105**, 82–88 (in Russian).

Piip V.B. 1984. New methods of interpreting of seismic time fields in media with variable velocities. *Moscow University Geology Bulletin* **3**, 86–95.

Piip V.B. 1991. Local reconstruction of seismic refraction sections on the basis of homogeneous functions. *Izvestiya, Academy of Sciences, USSR, Physics of Solid Earth* **27**, 844–850.

Piip V.B. and Efimova E.A. 1985. Definition of velocity field on the materials of engineering seismic prospecting. *Moscow University Geology Bulletin* **3**, 51–56.

Piip V.B. and Efimova E.A. 1987. The investigation of cross-sections with wave guides on the base of the medium model with homogeneous velocity function of the seismic waves. In: *Numerical Methods of Geophysics – Theory and Applications*, pp. 99–109. Scientific Works, Siberian Division of the Academy of Sciences of the USSR, Novosibirsk (in Russian).

Piip V.B. and Efimova E.A. 1990. Karst and near-surface structure on the base of a new refraction interpretation. 6th International IAEG Congress, Rotterdam, Expanded Abstracts, 1005–1008.

Piip V.B. and Efimova E.A. 1996. Investigation of deep structure of the Eastern European Platform using seismic refraction data. In: *Oil and Gas in Alpidic Thrustbelts and Basins of Central and Eastern Europe* (eds G. Wessely and W. Leibl), pp. 283–288. EAGE Special Publication 5.

Puzyrev N.N. 1963. On the theory of interpretation of individual seismic sounding. *Geologia i Geofizika* **9**, 85–99 (in Russian).

Zelt C.A. and Smith R.B. 1992. Seismic traveltime inversion for 2D crustal velocity structure. *Geophysical Journal International* **108**, 16–34.

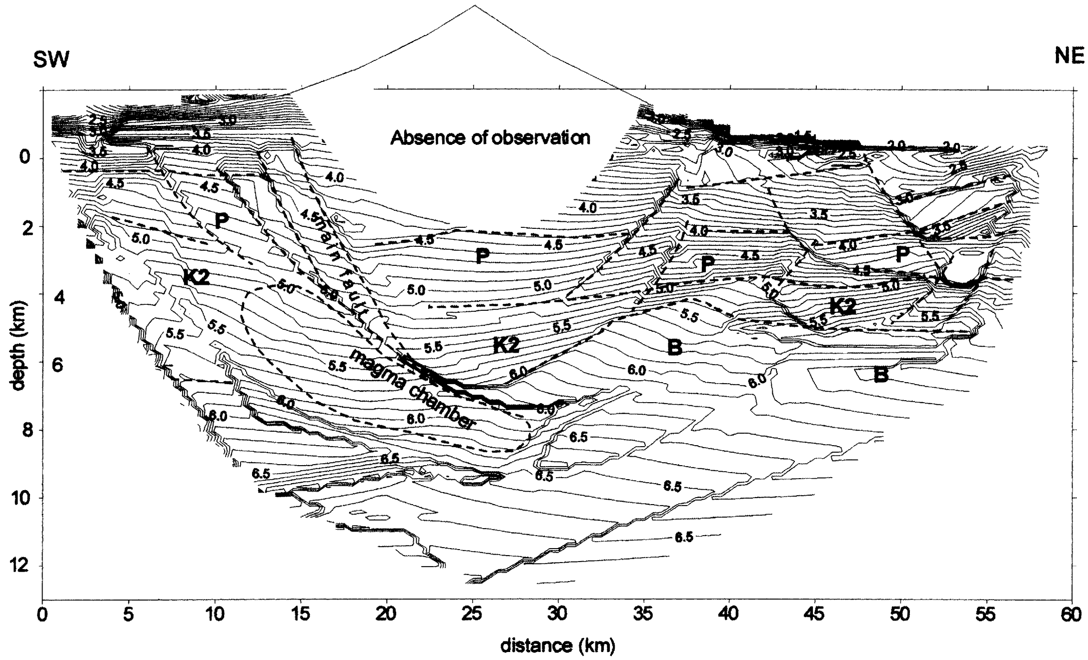

Figure 11 Seismic cross-section of the refraction data under the Kluchevskoy volcano and its geological interpretation. The thin lines indicate velocity contours. The contour interval is 0.1 km/s. The numbers indicate velocity values. The boundaries of layers and faults are shown by dashed lines. The presumed geological ages of the layers are indicated. The crystalline basement is denoted by the letter B. The presumed position of the magma chamber is indicated by a dashed line.

APPENDIX

Theory of the inversion method

Analysis of the eikonal equation using similarity theory methods

From the theory of similarity (Ehrenfest-Afanassjewa 1915), it is known that variables of differential or algebraic equations characterizing similar phenomena are invariant in linear transformations. An analysis of the eikonal equation using similarity theory methods distinguishes classes of velocity functions where time fields, seismic rays and traveltime curves characterize similarity relationships.

We consider the eikonal equation for a half-space given by the Cartesian coordinates (x,z) and a velocity that depends arbitrarily on two coordinates. This equation is

$$\left(\frac{\partial t}{\partial x}\right)^2 + \left(\frac{\partial t}{\partial z}\right)^2 = \frac{1}{v^2(x,z)}. \tag{A1}$$

The initial condition $t(x_0,z_0) = 0$ gives the location and time of a source. We introduce the following linear transformations of the variables:

$$x = C_1 x_1,$$
$$z = C_2 z_1, \tag{A2}$$
$$t = C_3 t_1,$$

where C_1, C_2, C_3 are constants. If

$$C_1 = C_2 \tag{A3}$$

and $v(x,z)$ is such that

$$v(C_1 x, C_1 z) = C_1^m v(x,z), \tag{A4}$$

and also if

$$C_3 = C_1^{1-m}, \tag{A5}$$

it is easy to prove that (A1) remains invariant and preserves the same form, i.e.

$$\left(\frac{\partial t_1}{\partial x_1}\right)^2 + \left(\frac{\partial t_1}{\partial z_1}\right)^2 = \frac{1}{v^2(x_1,z_1)}. \tag{A6}$$

Therefore time fields described by (A1) and the conditions (A2)–(A5) are similar. The condition (A4) distinguishes a class of homogeneous functions. According to the definition all homogeneous functions satisfy the following equation:

$$f(cx, cy) = c^m f(x,y),$$

where c is a constant and m is a power of the homogeneous function with the real values $-\infty < m < \infty$. In polar coordinates all homogeneous functions have the form,

$$v(r,\varphi) = r^m \psi(\varphi), \tag{A7}$$

where $\psi(\varphi)$ is an arbitrary function of the polar angle. Contours of homogeneous functions are similar curves, although the form of these contours is arbitrary. The defined domain of homogeneous velocity functions is $0 < r$, $0 \le \varphi \le \pi/2$, because for the point $r = 0$, $\varphi = 0$ the velocity value is zero, which does not make sense.

Wavefront and ray equations

In media with homogeneous velocity functions, rays crossing the same radius $\varphi = \varphi_0$ at the same angle $i = i_0$ are similar to each other. It is also found that there is a constant parameter or expression along the ray.

For a homogeneous velocity function, the differential equation of the ray can be reduced to a first-order equation. This can be shown as follows. The eikonal equation for a homogeneous velocity function in polar coordinates has the form,

$$\left(\frac{\partial t}{\partial r}\right)^2 + \frac{1}{r^2}\left(\frac{\partial t}{\partial \varphi}\right)^2 = \frac{1}{r^{2m}\psi^2(\varphi)}. \tag{A8}$$

This is a non-linear partial differential equation but it can be transformed into two ordinary differential equations. By substituting the following new variables in (A8):

$$T = r^{m-1}t, R = \ln r,$$

it is easy to obtain

$$\left(\frac{\partial T}{\partial R} - (m-1)T\right)^2 + \left(\frac{\partial T}{\partial \varphi}\right)^2 = \frac{1}{\psi^2(\varphi)}. \tag{A9}$$

Representing the solution as the sum of two functions,

$$T(R,\varphi) = V(R) + U(\varphi), \tag{A10}$$

and writing

$$\frac{\partial T}{\partial R} = q, \frac{\partial T}{\partial \varphi} = p, \tag{A11}$$

we obtain

$$\frac{q}{m-1} - V(R) = U(\varphi) \pm \frac{1}{(m-1)}\sqrt{\frac{1}{\psi^2} - p^2},$$

or

$$U(\varphi) \pm \frac{1}{(m-1)}\sqrt{\frac{1}{\psi^2} - p^2} = a, \tag{A12}$$

$$q/(m-1) - V(R) = a, \tag{A13}$$

where a is a constant of separation. It is easy to derive the solution of (A13)

$$V = C_1 e^{(m-1)R} - a.$$

We now consider (A12) for a ray given by polar coordinates (Fig. 12). It is known that $|\operatorname{grad} t| = 1/v$. The direction of the gradient coincides with the tangent to the ray. We introduce the angle i formed by the tangent to the ray with the normal to the line $\varphi =$ const line (Fig. 12). It can be shown that

$$\frac{1}{r}\frac{\partial t}{\partial \varphi} = \frac{\cos i}{v} = \frac{\cos i}{r^m \psi(\varphi)},$$

or

$$\frac{\partial T}{\partial \varphi} = \frac{\cos i}{\psi(\varphi)} = \frac{dU}{d\varphi} = p. \tag{A14}$$

Equation (A12) can be written as

$$\pm\frac{1}{(m-1)}\sqrt{\frac{1}{\psi^2(\varphi)} - \frac{\cos^2 i}{\psi^2(\varphi)}} + U(\varphi) = a.$$

The sign is determined by the direction of the angle i. If we choose the direction shown in Fig. 12, we obtain a positive sign and so we have

$$\frac{1}{(m-1)}\frac{\sin i}{\psi(\varphi)} + U(\varphi) = a, \tag{A15}$$

and hence

$$U(\varphi) = a - \frac{1}{(m-1)}\frac{\sin i}{\psi(\varphi)}.$$

We note here that the function ($\sin i$) depends on φ only. We now consider the function (A10),

$$T = U(\varphi) + V(R),$$

and obtain

$$T = -\frac{1}{(m-1)}\frac{\sin i}{\psi(\varphi)} + C_1 e^{(m-1)R}.$$

Using the variables (r,t), we find

$$r^{m-1}t = -\frac{1}{(m-1)}\frac{\sin i}{\psi(\varphi)} + C_1 r^{m-1}.$$

The constant C_1 may be found using the initial conditions $t(r_0,\varphi_0) = 0$, and thus

$$C_1 = \sin i_0/((m-1)\psi(\varphi_0)r_0^{m-1}).$$

We obtain

$$t = -\frac{1}{(m-1)}\frac{\sin i}{\psi(\varphi)r^{m-1}} + \frac{1}{(m-1)}\frac{\sin i_0}{\psi(\varphi_0)r_0^{m-1}}. \tag{A16}$$

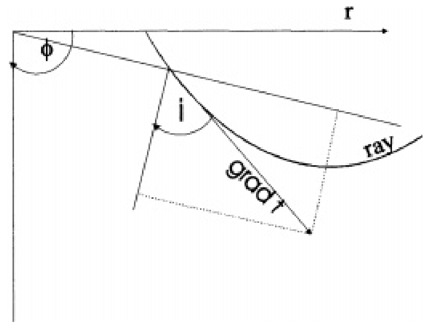

Figure 12 Seismic ray geometry in polar coordinates.

Function (A16) describes a time field in the medium with a homogeneous velocity function. This expression enables us to compute the initial angle i_0 of the ray at the source if we know the angle of emergence i and the arrival time t. Using (A7), we can write

$$(m-1)\,t = -\frac{r\sin i}{v} + \frac{r_0 \sin i_0}{v_0}. \tag{A17}$$

As

$$\frac{r_0 \sin i_0}{v_0} = \text{const},$$

the expression,

$$(m-1)t + r\sin(i)/v = p,$$

defines the value of the ray parameter p which remains constant along a ray.

Differential equation of a ray in media with a homogeneous velocity function

We now differentiate (A15) with respect to φ, and obtain

$$\frac{1}{(m-1)}\frac{\mathrm{d}}{\mathrm{d}\varphi}\left(\frac{\sin i}{\psi(\varphi)}\right) + \frac{\mathrm{d}U}{\mathrm{d}\varphi} = 0.$$

Using (A14), we can write

$$\frac{\mathrm{d}}{\mathrm{d}\varphi}\left(\frac{\sin i}{\psi(\varphi)}\right) = (1-m)\frac{\cos i}{\psi(\varphi)}. \tag{A18}$$

Equation (A18) is the differential equation of a ray in a medium with a homogeneous velocity function. We note that (A18) does not contain the variable r. It is an ordinary differential equation of the first order and its solution is of the form $i = i(\varphi, C)$, where C is defined by the initial condition $i_0 = i(\varphi_0, C)$. The solution of (A18) is invariant for any ray crossing the line $\varphi_0 = $ const at any point under angle $i_0 = $ const and therefore it describes a set of similar rays.

Similarity of wavefronts and traveltime curves

We write (A16) in the form

$$r^{m-1} t = -\frac{1}{(m-1)}\frac{\sin i}{\psi(\varphi)} + \frac{1}{(m-1)}\frac{\sin i_0}{\psi(\varphi_0)}\left(\frac{r}{r_0}\right)^{m-1},$$

and since sin i is a function of φ only (see (A15)), we can write

$$t = r^{1-m} F(\varphi, \varphi_0, r/r_0). \tag{A19}$$

We introduce the new variables,

$$R = r/r_0,$$

$$T = t/r_0^{1-m}, \tag{A20}$$

where r_0 is a radial coordinate of a source, and is constant. We then obtain

$$T = R^{1-m} F(\varphi, \varphi_0, R). \tag{A21}$$

Note that r_0 is not contained in (A21). As $r_0 = $ const, we have introduced a linear transformation (A20). Equation (A21) is invariant (see (A19)) with respect to (A20), therefore all time fields with sources located on the same radial line $\varphi_0 = $ const are similar to each other.

We illustrate this in the following way. We compute a time field $t_1(r_1, \varphi)$ with a source at the point $r_0 = r_{01}$, $\varphi = \varphi_0$ for a medium with velocity given by (A7) (henceforth referred to as medium (A7)). We input new coordinates,

$$T = t_1/r_{01}^{1-m}, R = r_1/r_{01}.$$

We obtain the time field $T(R, \varphi)$ which coincides numerically with a time field from a source located at point $r_0 = 1$, $\varphi = \varphi_0$ on the same radial line $\varphi = \varphi_0$, because if $r_1 = r_{01}$, then $R = R_0 \equiv 1$. In order to compute the time field $t_2 = t_2(r_2)$ with a source located at any other point on the same radial line, for instance $r_0 = r_{02}$, $\varphi = \varphi_0$, it is necessary to perform the following linear transformations,

$$r_2 = r_{02}R = (r_{02}/r_{01})r_1, \tag{A22}$$

$$t_2 = r_{02}^{1-m} T = (r_{02}/r_{01})^{1-m} t_1.$$

In order to obtain an equation of a traveltime curve system at the surface of the medium, we must substitute $\varphi_0 = 0$ (sources are at the surface) and $\varphi = 0$ (receivers are at the surface) in (A22). Thus the same equations (A22) are valid for refraction traveltime curves from any two sources at the surface of medium (A7). As the function $\psi(\varphi)$ is arbitrary, the medium (A7) can include velocity break lines or linear seismic boundaries and therefore the traveltime curve for this medium can be represented by three branches: direct, refraction and reflection traveltime curves. Equations (A22) are valid for them all and therefore for two reflection traveltime curves at the surface of medium (A7).

The transformations (A22) convert right-hand branches of any traveltime curve into right-hand branches of a traveltime curve from another source. This also holds for the left-hand branches, i.e. formulae (A22) are valid for the traveltime curves from adjacent shotpoints.

Transformation for two reverse traveltime curves

For media with velocity (A7), non-linear transformations of two reverse traveltime curves exist. They continuously map a forward traveltime curve on to the reverse one and vice versa. These transformations can be obtained using the reciprocity law. We consider a pair of reverse traveltime curves: a forward one $t_1(r_1)$ with source at the point r_{01} and the reverse one $t_2(r_2)$ with source at the point r_{02}, in the interval $[r_{01}, r_{02}]$ (Fig. 13).

According to the reciprocity law, $t_1(r_{02}) = t_2(r_{01})$. We examine an arbitrary point on the forward traveltime curve (t_1, r_1). We assume that the source r_0 of traveltime curve $t(r)$ is located at this point and thus $r_1 = r_0$. Obviously $t(r_{01}) = t_1(r_0)$ according to the reciprocity law. The traveltime curve $t(r)$ is obtained from a shotpoint adjacent to that of $t_2(r_2)$ and therefore $t(r)$ and $t_2(r_2)$ are similar to each other. Points on traveltime curve $t(r)$ can be transformed into points on traveltime curve $t_2(r_2)$ using (A22) and thus for the point (r_{01}, t) we obtain

$$r_2 = (r_{01}/r_0)r_{02},$$

$$t_2 = (t/r_0^{1-m})r_{02}^{1-m}.$$

As $r_0 = r_1$ and $t(r_{01}) = t_1(r_1)$, according to the reciprocity law we have

$$r_2 = \frac{r_{01}r_{02}}{r_1}, \qquad t_2 = \left(\frac{r_{02}}{r_1}\right)^{1-m} t_1. \tag{A23}$$

We obtain the point (t_2, r_2) on the reverse traveltime curve $t_2(r_2)$, corresponding to some point (t_1, r_1) on the forward traveltime curve $t_1(r_1)$ or an image (r_2, t_2) of point (t_1, r_1). These non-linear transformations are continuous.

Seismic boundaries, waveguides and layers with rapid increase of velocity can exist in the media being considered and, according to the presence or absence of signal, multivalues are expressed on pairs of reverse traveltime curves. The transformation (A23) results in the coincidence of all branches of the pair of reverse traveltime curves and it can therefore be used for the identification of waves from different boundaries on pairs of reverse traveltime curves.

Transformation of the eikonal equation for velocity (A7) to the eikonal equation for velocity depending on the polar angle: reducing the dimension of the problem

The medium with velocity (A7) is a 2D inhomogeneous medium, with velocity depending significantly on two coordinates. However, forward and inverse problems in this medium can be converted to 1D problems.

In the eikonal equation (A8), we substitute

$$\rho = r^{1-m}, \qquad \alpha = |1 - m|\varphi, \qquad \tau = |1 - m|t, \tag{A24}$$

and obtain

$$\left(\frac{\partial \tau}{\partial \rho}\right)^2 + \frac{1}{\rho^2}\left(\frac{\partial \tau}{\partial \varphi}\right)^2 = \frac{1}{\psi^2(\alpha/|1 - m|)} = \frac{1}{\xi^2(\alpha)}. \tag{A25}$$

This is the eikonal equation in polar coordinates for velocity depending on the polar angle only, i.e. a 1D velocity function. Equations (A24) will transform the forward and inverse problem for media (A7) to the 1D case, simplifying them significantly. However, in the case of $m = 1$ the transformations do not make sense. This is a special point and is excluded from our examination. It has been investigated by Piip (1982b).

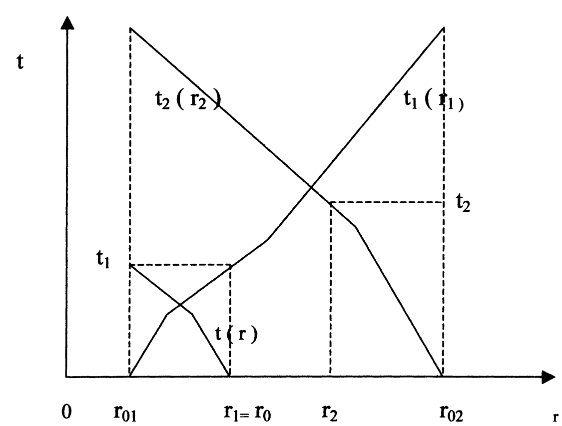

Figure 13 Transformations of two reverse traveltime curves.

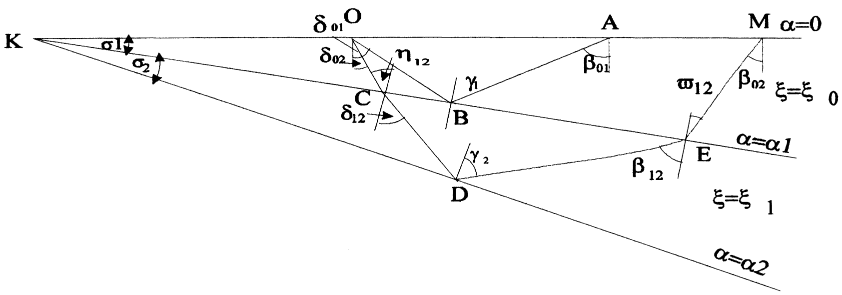

Figure 14 Ray propagation geometry.

Inverse kinematics problem: reconstruction of a homogeneous velocity function in two coordinates from the data of a pair of reverse first-arrival traveltime curves

We assume that we have a pair of reverse first-arrival traveltime curves: $t_1(x_1)$ from a source at the point x_{01} and $t_2(x_2)$ from a source at the point x_{02}, given in the interval $[x_{01},x_{02}]$. We also assume that the real velocity distribution can be approximated by function (A7). We do not know the values of the polar coordinates for the given traveltime curves. We assume that the polar origin is located at an unknown point on the profile, either to the right or to the left of the interval $[x_{01},x_{02}]$. Therefore for $\varphi = 0$, we have $r = |x + c|$, where c is an unknown constant. Values of the polar coordinates may be defined by the formulae,

$$r = \sqrt{(x + c)^2 + z^2},$$
$$\varphi = \arctan\left(\frac{z}{|z + c|}\right),$$

and the velocity function may be written

$$v = \left(\sqrt{(x + c)^2 + z^2}\right)^m \psi\left(\arctan\left(\frac{z}{|x + c|}\right)\right), \tag{A26}$$

where m and c and the values of the function $\psi(\varphi)$ are unknown. It is necessary to restrict the defined domain of the unknown parameters m and c. Experience has shown that m should lie in the range $-2 \le m \le 2$. The restrictions on c may be obtained from a system of inequalities $x_{01} + c > 0$ and $x_{02} + c > 0$, or $x_{01} + c < 0$ and $x_{02} + c < 0$, so that the origin $r = 0$ does not lie within the interval $[x_{01},x_{02}]$. Thus we obtain the conditions $c > -x_{01}$ or $c < -x_{02}$.

We know that for medium (A7), a forward traveltime curve can be transformed into the reverse one using (A23). In Cartesian coordinates the transformations (A23) have the form,

$$x_2 + c = \frac{(x_{01} + c)(x_{02} + c)}{x_1 + c}, \tag{A27}$$

$$t_2 = \left(\frac{x_{02} + c}{x_1 + c}\right)^{1-m} t_1.$$

We use these transformations to compute m and c. We compute the mean square deviation between the observed forward traveltime curve and the transformed reverse curve using (A27) for arbitrary values of m and c. The function f of m and c can be obtained if the observed time values are known at n points. It is given by

$$f(c, m) = \frac{1}{n}\left(\sum_{i=1}^{n}(t_1(x_{1i}) - t_1^s(x_{1i}))^2\right),$$

where (A28)

$$t_1^s(x_{1i}) = \left(\frac{x_{1i} + c}{x_{02} + c}\right)^{1-m} t_2\left(\frac{(x_{01} + c)(x_{02} + c)}{x_{1i} + c} - c\right).$$

The function $f(c,m)$ is now minimized using standard algorithms for minimizing a function of several variables. The values of m and c which give a minimum value of $f(c,m)$ are taken as the parameters of the unknown velocity function.

We now compute the mean (approximate) traveltime curve corresponding to an unknown approximate velocity function. We convert the observed traveltime curves to polar coordinates using the computed value of c, so that

$$r = |x + c|,$$

and then we transform the observed reverse traveltime curve $t_2(r)$ into the forward one using (A23), and the calculated values of m and c. We obtain

$$t_1^s(r) = \left(\frac{r}{r_{02}}\right)^{1-m} t_2\left(\frac{r_{01}\, r_{02}}{r}\right).$$

We compute the mean traveltime curve $\bar{t}(r)$ using the formula,

$$\bar{t}(r) = \tfrac{1}{2}\left(t_1(r) + t_1^s(r)\right).$$

We assume that $\bar{t}(r)$ corresponds to some velocity function (A7), while the function $\psi(\varphi)$ remains unknown for the present. We then convert the 2D problem to a 1D problem. We transform the mean traveltime curve $\bar{t}(r)$ using (A24), so that we obtain

$$\tau = |1 - m|\bar{t},$$

$$\rho = r^{1-m},$$

$$\rho_0 = r_{01}^{1-m}.$$

Finally, we obtain the traveltime curve $\tau(\rho)$ with source at the point ρ_0, corresponding to the unknown velocity function $\xi = \xi(\alpha)$.

Form of a traveltime curve $\tau(\rho)$ in a medium with velocity $\xi = \xi(\alpha)$

We require a function $\xi = \xi(\alpha)$ that is an increasing function of the polar angle α. We know that in the case of a velocity increasing with depth z, the traveltime curve is convex, so before computing $V(z)$ the traveltime curve must be approximated by a convex curve. We show that if the velocity is an increasing function of the polar angle, the traveltime curve is also convex.

In the medium with velocity (A7), rays have the parameter given by (A17). In the case $m = 0$, the source and receiver are located at the surface $\varphi = 0$ at the points ρ_0 and ρ and therefore $\xi = \xi_0$. The parameter is given by the expression,

$$-\ \tau = \frac{\sin i_0}{\xi_0}\rho_0 - \frac{\sin i}{\xi_0}\rho.$$

This gives

$$\begin{aligned} \frac{\partial\tau}{\partial\rho} &= \frac{\sin i}{\xi_0}, \\ \sin i_0 &= \frac{\xi_0}{\rho_0}\frac{\partial\tau}{\partial\rho}\rho - \frac{\xi_0}{\rho_0}\tau. \end{aligned} \tag{A29}$$

We differentiate (A29) with respect to ρ and obtain

$$\frac{\partial\,(\sin i_0)}{\partial\rho} = \frac{\xi_0}{\rho_0}\frac{\partial^2\tau}{\partial\rho^2}\rho + \frac{\xi_0}{\rho_0}\frac{\partial\tau}{\partial\rho} - \frac{\xi_0}{\rho_0}\frac{\partial\tau}{\partial\rho}.$$

We define the sign of the left- and right-hand sides of the equation:

$$\mathrm{sgn}\left(\frac{\partial i_0}{\partial\rho}\right) = \mathrm{sgn}\left(\frac{\partial^2\tau}{\partial\rho^2}\right),$$

and then we have

$$\text{if } \frac{\partial i_0}{\partial\rho} > 0 \Rightarrow k > 0,$$

$$\text{and if } \frac{\partial i_0}{\partial\rho} < 0 \Rightarrow k < 0,$$

where k denotes the curvature of the traveltime curve $\tau(\rho)$. If the initial angle i_0 decreases with increasing distance ρ, then we have a direct branch of the traveltime curve, which is convex. Therefore direct branches of traveltime curve $\tau(\rho)$ are convex. If the angle i_0 increases with increasing distance ρ, then we have an inverse branch of the traveltime curve $\tau(\rho)$, which is concave. This means that inverse branches of traveltime curve $\tau(\rho)$ are concave when multivalued and cusps exist on $\tau(\rho)$. If we assume that the rays do not intersect in the medium, the traveltime curve is convex and we must approximate it by a convex curve to compute the increasing function $\xi(\alpha)$.

Computation of the function $\xi = \xi(\alpha)$

In order to obtain the velocity $\xi = \xi(\alpha)$ as an unknown continuous increasing function and simultaneously to find boundaries, we replaced $\xi = \xi(\alpha)$ by a step function,

$$\xi^*(\alpha) = \begin{cases} \xi_0(0 \le \alpha \le \alpha_1) \\ \xi_1(\alpha_1 \le \alpha \le \alpha_2) \\ \quad \cdots\cdots\cdots \\ \quad \xi_n(\alpha_n \le \alpha) \end{cases}, \tag{A30}$$

where

$$\{\xi_{i+1} > \xi_i\}_{i=0}^{n}.$$

Since $\xi^*(\alpha)$ is a function of the polar angle, the elementary layers are wedge-shaped with constant velocities $\xi = \xi_i$. In this medium with velocity (A30), only head waves exist and the traveltime curve of the first arrival is a broken line consisting of linear traveltime curves of elementary head waves. We make the following assumptions: that the traveltime curve $\tau(\rho)$ is given at n discrete points $\{\rho_k, \tau_k\}_{k=0}^{n}$, where n is the number of interpolation points on $\tau(\rho)$; that every point on $\tau(\rho)$ is the initial point of a head wave; that the unknown medium with velocity (A30) contains n layers. This data is used to calculate the velocities ξ_i and the angles $\sigma_i = \alpha_{i+1} - \alpha_i$ *of* the wedge-shaped layers. The rays are indicated by the index k: $\{k\}_{i=0}^{n}$, and the boundaries between the layers by the index l:$\{l\}_{i=0}^{n}$. The angle of each layer is denoted by σ_l. The rays are refracted at every boundary and if the angle of refraction is critical, a head wave occurs. We consider only those rays which are reflected from the boundaries at the critical angle (Fig. 14). Angles of emergence of the rays at the boundary l are denoted by $\beta_{l\,k}$. The initial angles at the same boundary are denoted by $\delta_{l\,k}$ and the critical angle for this boundary is denoted by γ_l. The velocity in the first layer is defined by

$$\xi_0 = \frac{1}{\partial\tau/\partial\rho}\bigg|_{\rho=\rho_0}.$$

In order to define the angles of emergence of the rays at the surface, we differentiate and obtain

$$\left\{\beta_{0k} = \arcsin\left(\xi_0 \frac{\partial\tau}{\partial\rho}\bigg|_{\rho=\rho_k}\right)\right\}_{k=1}^{n}.$$

The initial angles are defined using the expression for the ray parameter (A17) which for this case can be written

$$-\tau_k = \frac{\sin\delta_{0k}}{\xi_0}\rho_0 - \frac{\sin\beta_{0k}}{\xi_0}\rho_k.$$

We thus obtain

$$\left\{\delta_{0k} = \arcsin\left(\frac{\xi_0}{\rho_0}\left(\frac{\sin\beta_{0k}}{\xi_0}\rho_k - \tau_k\right)\right)\right\}_{k=1}^{n}.$$

From triangles KOB and KAB (Fig. 14), we obtain

$$\sigma_1 = \frac{\beta_{01} - \delta_{01}}{2}, \qquad \text{(A31)}$$

$$\gamma_1 = \frac{\delta_{01} + \beta_{01}}{2},$$

and then

$$\xi_1 = \frac{\xi_0}{\sin\gamma_1},$$

where γ_1 is the critical angle. Formulae similar to (A31) were derived by Adachi (1954). Thus the angle σ_1 of the first layer and the velocity value ξ_1 in the second layer have been computed and the recursive method is now applied. All rays are continued downwards at the first boundary $l = 1$, i.e. the top of the second layer. We will compute the angles of emergence of the rays and the initial angles $\{\delta_{1k}\}_{k=2}^{n}, \{\beta_{1k}\}_{k=2}^{n}$ t the boundary $l = 1$ of the layer with velocity $\xi = \xi_1$.

For this we introduce the angles of incidence of rays at the boundary l=1:

$$\eta_{12}, \omega_{12},$$

$$\{\eta_{1k}\}_{k=2}^{n}, \{\omega_{1k}\}_{k=2}^{n}$$

(see Fig. 14).

From triangles KOC and KEM (Fig. 14), we obtain

$$\eta_{12} = \sigma_1 + \delta_{02},$$

and by analogy for other points on the traveltime curve,

$$\{\eta_{1k} = \sigma_1 + \delta_{0k}\}_{k=2}^{n},$$

and

$$\omega_{12} = \beta_{02} - \sigma_1,$$

$$\{\omega_{1k} = \beta_{0k} - \sigma_1\}_{k=2}^{n}.$$

We write the law of refraction for boundary $l = 1$:

$$\frac{\sin\eta_{1k}}{\sin\delta_{1k}} = \frac{\xi_0}{\xi_1}, \frac{\sin\omega_{1k}}{\sin\beta_{1k}} = \frac{\xi_0}{\xi_1},$$

and by analogy, for all points we can write:

$$\left\{\delta_{1k} = \arcsin\left(\frac{\xi_1}{\xi_0}\sin\eta_{1k}\right)\right\}_{k=2}^{n},$$

$$\left\{\beta_{1k} = \arcsin\left(\frac{\xi_1}{\xi_0}\sin\omega_{1k}\right)_{k=2}^{n}.\right.$$

We have now found the initial angles and angles of emergence of all rays for the second layer. The process can be repeated. The angle of the second layer, the critical angle and the velocity in the third layer can be defined by:

$$\sigma_2 = \frac{\beta_{12} - \delta_{12}}{2},$$

$$\gamma_2 = \frac{\beta_{12} + \delta_{12}}{2},$$

$$\xi_2 = \frac{\xi_1}{\sin\gamma_2}.$$

By repeating the computing down to the last layer, we compute the table of values for the function $\xi(\alpha)$:

$$\left\{\alpha_i = \sum_{i=1}^{i}\sigma_i, \qquad \xi = \xi_i\right\}_{i=0}^{n}.$$

Thus we have defined the function $\xi(\alpha)$. We now return to the original coordinates,

$$r = \rho^{1/(1-m)},$$

$$\varphi = \frac{\alpha}{|1 - m|},$$

$$\psi = \xi,$$

and compute the velocity function.

In the process of computing the function $\xi(\alpha)$ we have calculated the rays. It should be noted that the last ray (the boundary ray) to restrict the domain of the cross-section is where the real velocity distribution corresponds to the derived function.